VALIDATION OF A PEDESTRIAN SEDAN BUCK USING A HUMAN FINITE ELEMENT MODEL

Shunji Suzuki
Yukou Takahashi,
Masayoshi Okamoto
Honda R&D Co., Ltd.,
Japan

Rikard Fredriksson
Autoliv Research
Sweden

Shinsuke Oda
Autoliv Japan Ltd.,
Japan
Paper Number 11-0277

ABSTRACT

For the purpose of reproducing complex vehicle-pedestrian interactions using a simplified and standardized vehicle model, a previous study has developed a computational model for a generic buck to reproduce car-small sedan interaction using a standardized vehicle front model. Although the previous study validated the buck model using a finite element (FE) model for a pedestrian dummy in terms of pedestrian kinematics and vehicle-pedestrian contact forces, the buck structure has not been further validated with regard to responses of injury measures against a more biofidelic tool such as a human FE model.
The objective of this study was to evaluate the buck model representing a small sedan developed in the previous study (Untaroiu et al., ESV 2009) against a human FE model in terms of pedestrian kinematics and injury measures from comparisons between the buck and full vehicle models.
A human FE model developed by Takahashi et al. (IRCOBI 2010) was used in the current study. For the purpose of validating the buck model, an FE vehicle model representing the same small sedan was also used for comparisons. The pedestrian model was hit by the center of both vehicle models laterally at a baseline impact velocity of 40 km/h used by the previous study. In order to evaluate robustness of the buck model against impact velocity, impact simulations were performed at 20 and 60 km/h as well.
The results of the comparisons showed that the pedestrian kinematics and values of injury parameters were generally well reproduced by the buck model compared to the vehicle model. It was also found that for enhanced representation of the responses of injury measures to the pelvis and lower limb, some modifications to the buck components are suggested in terms of geometry, material property and structure.

INTRUDUCTION

The percentage of pedestrian fatalities in traffic accidents is considerably high worldwide from OECD data sets (International Traffic Safety Data and Analysis Group, 2010). Pedestrian fatalities account for over one thousand annually in USA (4378 people, 12% of all road user fatalities), Korea (2137, 36%), Japan (2012, 35%) and Poland (1467, 32%). Especially in Japan, the percentage of pedestrian fatalities exceeds that of vehicle occupants (21%). Therefore, a demand for pedestrian safety technology is increasing to provide safer environments for vulnerable road users.
A study done by IHRA (International Harmonized Research Activity) (Mizuno 2005) showed that in severe injuries to pedestrians, the percentage of lower extremity is one of the highest of all body regions, with severe injury defined as Abbreviated Injury Scale (AIS) 2-6. In the following three countries, the lower extremity accounted for the highest percentage of all body regions (39% in USA from Pedestrian Crash Data Study (PCDS) between 1994 and 1999, 40% in Germany from German In-Depth Accident Study (GIDAS) between 1985 and 1998, 42% in Japan from collected data by Japan Automobile Research Institute (JARI) between 1987 and 1988 and by Institute for Traffic Accident Research and Data Analysis (ITARDA) 1994 and 1998). In Australia, the lower extremity accounted for the second highest percentage (31%) from at-the-scene investigations of pedestrian collisions in the Adelaide metropolitan area in 1999 and 2000. The data from these countries show high priority of

lower extremity protection.
Among lower extremity injuries, pelvic fracture is most important from a viewpoint of threat to life, because pelvic fracture links to a substantial factor in pedestrian morbidity and mortality (Eastridge et al. 1997). Pelvic fracture may cause high blood loss because of the arteries located inside of pelvic ring.
Research for the relationship between pedestrian pelvic fracture and vehicle shape was made by Snedeker et al. (2003, 2005). Takahashi et al. (2010) analyzed pelvic injury patterns due to car-pedestrian collisions and identified three different impact locations relative to the pelvis that lead to different loading mechanisms. These studies analyzed details of pelvis injury mechanism using human FE models and vehicle models to investigate the effect of vehicle front geometry on injury parameters. However, the effect of vehicle stiffness characteristics has not been investigated.
Untaroiu et al. (2009) developed FE pedestrian sedan buck models representing a mid-sized sedan and a large sedan to investigate the influence of vehicle front end structures on pedestrian kinematics and loading. Although the buck models were validated using POLAR II (Akiyama et al. 2001) FE model by comparing pedestrian dummy kinematics and reaction forces with the results of impact simulations using vehicle FE models, the buck models have not been validated in terms of injury parameters.
In this study, injury levels exerted on the pelvis and lower limb along with whole-body kinematics were evaluated using the human FE model developed by Takahashi et al. (2010) by performing car-pedestrian impact simulations using the mid-sized sedan buck model proposed by Untaroiu et al. and a vehicle FE model. Pelvis deformation, femur bending moment, MCL (Medial Collateral Ligament) tensile strain and tibia bending moment were chosen as injury parameters. Pedestrian kinematics was also compared. In addition, the influence of impact velocity was also evaluated by changing the impact velocity.

METHODOLOGY

Human FE Model

In the current study, all the FE simulations were run using PAM-CRASH. The human FE model used in this study was developed by Takahashi et al. (2010). The model represents a mid-sized male anthropometry. The FE lower limb model was extensively validated against numerous published human data as presented by Kikuchi et al. (2006). The pelvis model was validated against the results of the dynamic lateral loading tests using isolated human pelves performed by Salzar et al. (2008). The upper part of the body was represented using articulated rigid bodies with the neck and lumbar models divided into seven and five segments, respectively, to represent flexibility of these regions in a biofidelic manner. The kinematics of the full body model was validated in sedan and SUV impacts as performed by Kikuchi et al. (2008), confirming that all the trajectories were within the trajectory corridors developed using the data from published full-scale car-pedestrian impact tests using human surrogates.

Car-Pedestrian Impact Simulations

The pedestrian model was hit laterally from the left by the center of an FE vehicle model and an FE buck model. Figure 1 shows the simulation models for a vehicle model representing a mid-sized sedan and a buck model simulating the vehicle developed by Untaroiu et al. (2009) at the time of initial contact. A gravitational field was applied to the pedestrian model. The lower limbs were rotated about the latero-medial axis by ten degrees with the right limb forward to represent a gait stance. A baseline impact velocity was chosen at 40 km/h as this velocity is used as the standard velocity in regulations and new car assessment programs worldwide. Real world pedestrian accident data show that cumulative frequency of pedestrian accidents is over 90% at 60 km/h in USA, Japan, Germany and Australia (Mizuno 2005). For this reason, in addition to 40 km/h impact, 20 km/h and 60 km/h were also chosen for evaluating robustness of the buck performance against impact velocity.

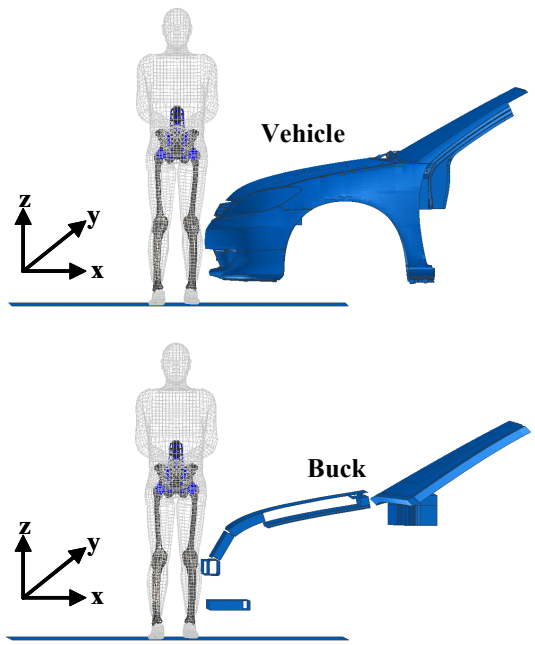

Figure 1. Full scale impact simulation models for mid-size sedan vehicle and buck models.

Injury Parameters

Some injury parameters that correlate with pelvis and lower limb injuries were compared between the full-vehicle and buck models. Ikeda et al. (2010) investigated injury indices for pelvic fracture using a human FE model, and found that lateral compression of the pelvis is the best predictor of pubic rami fracture. Based on this finding, the current study used deformation between the left and right acetabulum for pubic rami fracture as shown in Figure 2. Femur and tibia bending moment were used as injury measures for fracture of these bones. The locations of the cross-sections at which bending moment was recorded are presented in Figure 2. Five and three sections were chosen on the femur and tibia of the struck-side, respectively. Since maximum bending moment was always seen at the distal and proximal cross-sections of the femur and tibia, respectively, only the moment time histories at these cross-sections were used for the analysis. Tensile strain was used as an injury measure for failure of the knee ligaments. Although tensile strain generated at every ligament was recorded, only MCL strain was used in the analysis since maximum strain was always generated in the MCL. Figure 3 shows the locations of the datum points from which MCL tensile strain was calculated.

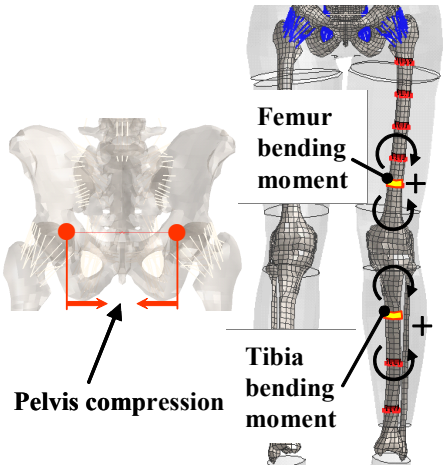

Figure 2. Measurement locations for pelvis deformation, femur and tibia bending moment.

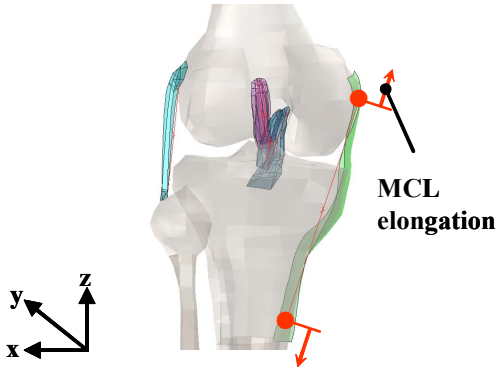

Figure 3. Datum point for MCL tensile strain.

Kinematics

Untaroiu et al. (2009) compared trajectories of the head CG (Center of Gravity), T1 (1st thoracic vertebra), T8 (8th thoracic vertebra) and pelvis of the POLAR II FE model between the vehicle and buck FE models. These locations were used to develop trajectory corridors from full-scale car-pedestrian impact tests using human surrogates for determining performance specifications of pedestrian dummies (J2868 SAE information report). In this study, the same procedure was applied to compare kinematics of the human model between the vehicle and buck FE models.

RESULTS

Injury parameters and kinematics at 40km/h

Figure 4 shows the time history responses of injury parameters generated on the human FE model. Positive pelvis deformation corresponds to decrease in the distance between the datum points defined in Figure 2 (compression). Close magnitude is shown for both the vehicle model and the buck model until 11 ms. After 11 ms up to 32 ms, the result from the vehicle model shows larger pelvis deformation than that from the buck model. At 32 ms, pelvis deformation from both models becomes close again. After 32 ms, the result from the buck model shows larger deformation than that from the vehicle model.

Positive femur bending moment corresponds to femur bending convex to the medial side of the pedestrian. General trend is similar to that of pelvis deformation. Femur bending moment is close between the vehicle and buck models until 9 ms. After 9 ms up to 17 ms, the result from the vehicle model shows smaller femur bending moment than that from the buck model. From 17 ms to 29 ms, close femur moment is shown between both models. After 29 ms, femur moment is larger with the buck model.

As for MCL tensile strain, the vehicle model shows negative strain up to 5 ms but the buck model shows almost no strain up to 3 ms. After 3 ms, both models show increase in MCL strain. Always the buck model shows larger strain than the vehicle model.

Positive tibia bending moment is defined in the same manner as femur moment. Tibia bending moment from both models shows no increase until 6 ms. The result from the buck model shows increase in tibia moment after 6 ms. The result from the vehicle model shows negative peak value at 8 ms and then starts to increase. Between 6 ms and 18 ms, the result from the buck model shows higher moment than that from the vehicle model.

Figure 5 compares trajectories from the human FE model between initial contact to 130 ms. This

termination time was chosen because at this timing the head contacted the windshield with the vehicle model, which was slightly earlier than that for the buck model. Thin lines represent vehicle model results and thick lines show buck model results. Overall, the trajectories match well between the results from the vehicle and buck models, with maximum difference at 130 ms 69 mm for head z-displacement and 41 mm for pelvis x-displacement.

Effect of impact velocity change on injury parameters and kinematics

Figures 6 and 8 compare injury parameter time histories at 20 km/h, 40 km/h and 60 km/h for the vehicle and buck models, respectively. Table 1 summarizes the comparison of the difference in peak injury measures between 20 km/h and 40 km/h and between 40 km/h and 60 km/h. No evident positive peaks of pelvis deformation are identified for the vehicle model. In contrast, both negative and positive peaks of pelvis deformation are seen with the buck model. For this reason, negative peaks of pelvis deformation (pelvis tension) identified for both the vehicle and buck models were compared in Table 1. As for femur bending moment, both negative and positive peaks are identified for both the vehicle and buck models. Overall peaks of femur bending moment are reached on a positive side for all cases except the vehicle model result at 60 km/h. In addition, positive peaks are due to direct contact of the vehicle front structure with the thigh, while initial negative peaks are primarily due to loading to the leg and knee. For this reason, positive peaks of femur bending moment are compared in Table 1.
The differences between vehicle and buck models are not significant with the MCL tensile strain and tibia bending moment. As for the pelvis deformation, a larger difference between vehicle and buck models are seen when impact velocity is changed from 20 km/h to 40 km/h. In contrast, for femur bending moment, the difference between the vehicle and buck models is more evident when impact velocity is changed from 40 to 60 km/h.
Figures 7 and 9 compare full-body kinematics between 20 km/h, 40 km/h and 60 km/h for the vehicle and buck models, respectively. Similar general trends are seen for both vehicle and buck models. For all trajectories, the horizontal coordinates at 130 ms increased as the impact velocity increased.

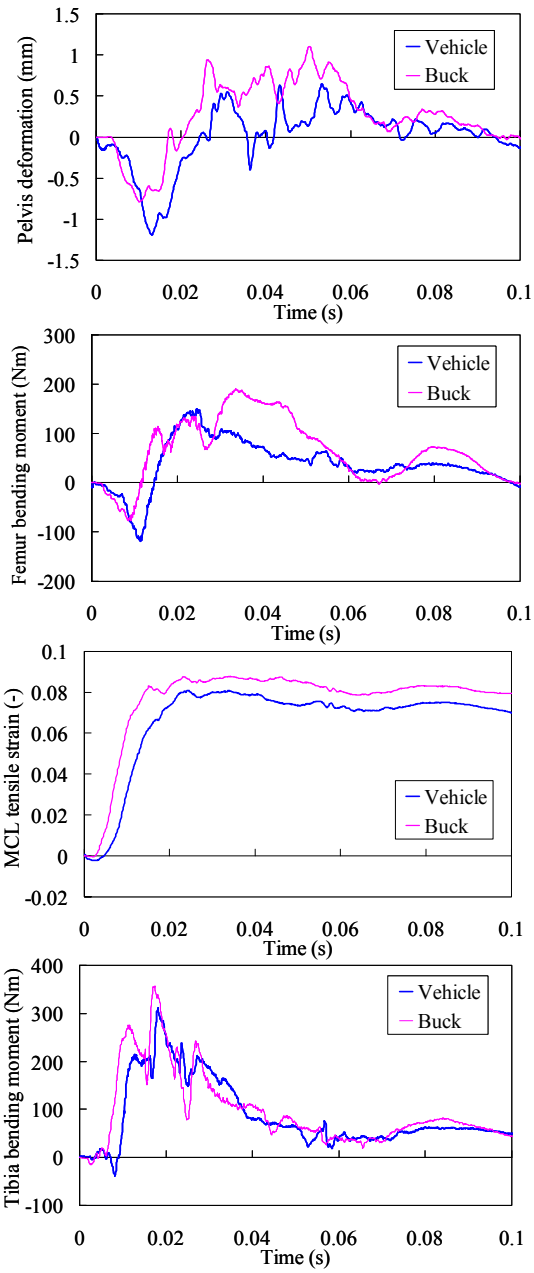

Figure 4. Comparison of time histories of injury parameters between vehicle and buck models.

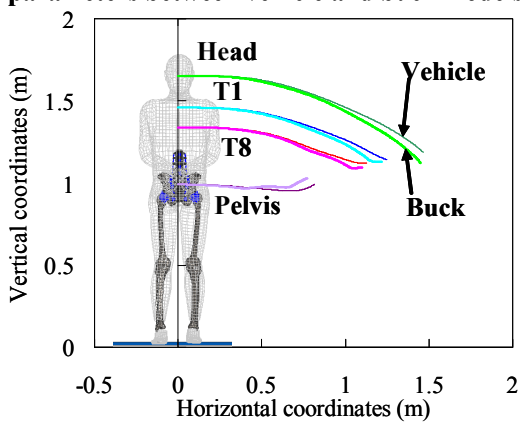

Figure 5. Comparison of full-body kinematics between vehicle and buck models.

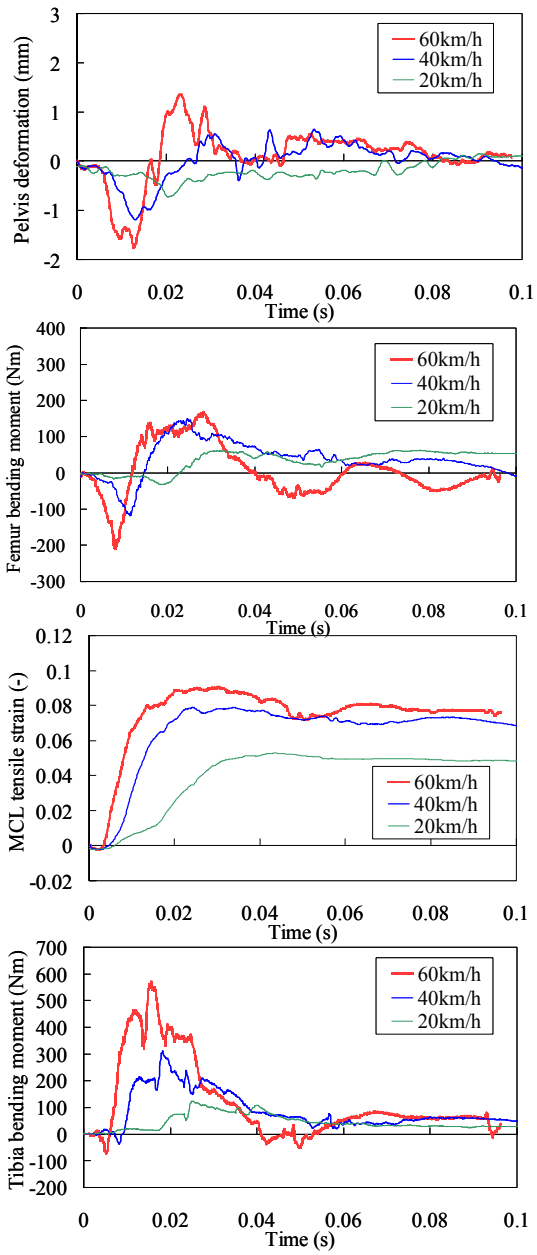

Figure 6 . Comparison of injury parameter time histories between 20 km/h, 40 km/h and 60km/h for vehicle model.

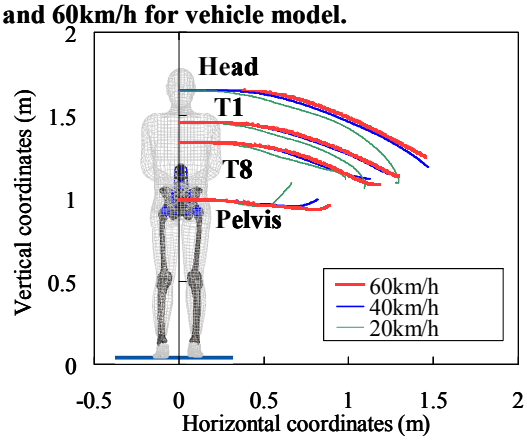

Figure 7 . Comparison of full-body kinematics between 20 km/h, 40 km/h and 60km/h for vehicle model.

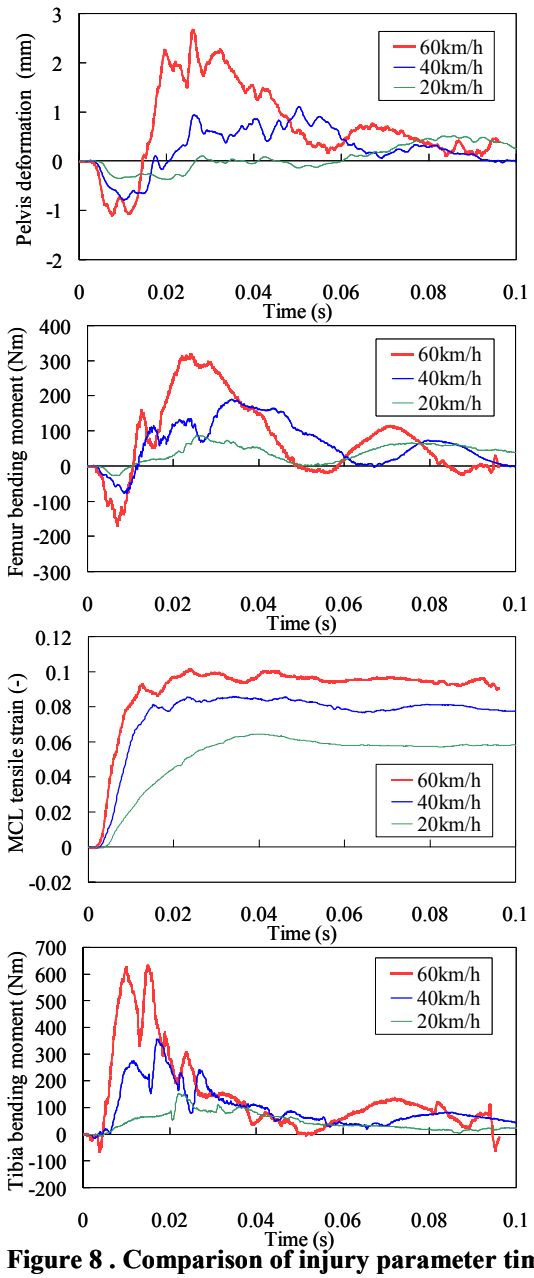

Figure 8 . Comparison of injury parameter time histories between 20 km/ h, 40 km/h and 60 km/h for buck model.

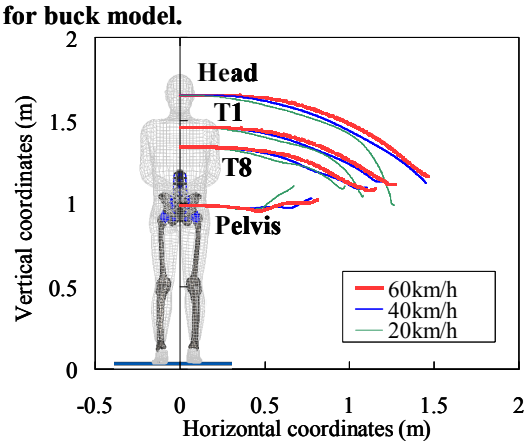

Figure 9. Comparison of full-body kinematics between 20 km/h, 40 km/h and 60 km/h for buck model.

Table 1 . Comparison of maximum injury parameters ratio from 20 km/h to 40km/h and from 40 km/h to 60km/h

	Pelvis tension		Femur bending moment		MCL tensile strain		Tibia bending moment	
	Vehicle	Buck	Vehicle	Buck	Vehicle	Buck	Vehicle	Buck
20 → 40km/h	165	214	246	219	149	133	115	118
40 → 60km/h	147	139	111	168	249	233	184	177

Unit:%

DISCUSSION

For designing bucks for reproducing car-pedestrian impact, characteristics of loading from the buck to a pedestrian (magnitude, location and timing) are key factors that determine pedestrian injury value and kinematics. Based on this understanding, the effect of the difference in loadings applied to a pedestrian on pedestrian impact responses is discussed.

Since difference in pedestrian kinematics was not significant between the vehicle and the buck in 40 km/h impact, the effect of difference in pedestrian loadings on injury parameters is investigated at this impact velocity. In impact velocity changes from 20 km/h to 40 km/h and from 40 km/h to 60 km/h, similar change in pedestrian kinematics was identified between the vehicle and buck models. In addition, no significant difference in the change of peak MCL tensile strain and tibia bending moment was seen. Therefore, the effect of impact velocity change on negative peak of pelvis deformation and positive peak of femur bending moment is discussed in this section.

Difference in impact force time histories

Difference in injury parameters at 40km/h.

Figure 10 shows the center cross-sections of the vehicle and buck models. In order to investigate onset timing of impact force, all dimensions in x-direction were measured relative to the front end of the bumper face. In order to investigate location of point of application of the force relative to the pedestrian, all dimensions in z-direction were measured relative to the ground level. Since injury is normally assessed by the maximum value of injury parameters, difference of injury parameters was analyzed up to the timing when maximum value was reached.

Figure 11 shows impact force time histories of the hood, grille, bumper face and bumper lower of the vehicle and buck models. The ratios of z-component to x-component of the impact force from the hood, grille, bumper face and bumper lower were 63%, 33%, 18% and 31%, respectively, from a preliminary analysis. Since the ratio of z-component of the impact force was exceptionally large for the hood, both x-component and z-component were compared for the hood, while only x-component was compared for the grille, bumper face and bumper lower.

Impact force time histories from the hood, grille, bumper face and bumper lower obtained from impact simulations using the vehicle and buck models were classified into four time phases, depending on the difference in loading configuration and magnitude between the vehicle and buck models.

Phase-I: From initial contact up to 5 ms, both the bumper face and bumper lower contacted the lower limb for the vehicle model. In contrast, only the bumper face contacted the lower limb for the buck model. This difference resulted in larger MCL tensile strain for the buck model due to larger rotation of the leg underneath the bumper caused by the lack of loading from the bumper lower. This can be attributed to difference in horizontal location of the bumper lower of the buck model from that of the vehicle model (9 mm difference as shown in Figure 10).

Phase-II: Between 5 ms and 13 ms, two major differences in pedestrian loading situation were identified. The first one is that the grille along with the bumper face and bumper lower applied load to the pedestrian for the vehicle model, while only the bumper face and bumper lower contacted the pedestrian for the buck model. This difference in loading configuration resulted in difference in further difference in MCL tensile strain due to the lack of contact of the thigh with the grille for the buck model, which would yield larger rotation of the thigh. The difference in loading configuration also yielded less impact force applied from the buck model to the distal thigh, resulting in 1) less tensile force at the hip joint and thus earlier shift of pelvis deformation from tension (negative) to compression (positive) and 2) earlier shift of femur moment from negative to positive. The difference in loading configuration can be attributed to difference in horizontal location of the front end of the grille between the vehicle and buck models (9 mm difference as shown in Figure 10).

The second major difference in pedestrian loading situation is that the magnitude of impact force from the bumper face was larger for the buck model, while that from the bumper lower was larger for the vehicle model. Due to higher force from the bumper face of the buck model, tibia bending moment was also higher with the buck model. The lower impact force from the bumper lower of the buck model, along with the previously mentioned

difference, resulted in higher MCL tensile strain due to larger rotation of the leg underneath the bumper. These differences can be attributed to difference in structure and material property of the bumper face and bumper lower, and horizontal location of the front end of the bumper beam between the vehicle and buck models (20 mm difference as shown in Figure 10).

Phase-III: Between approximately 25 ms and 42 ms, both the grille (in x-direction) and the hood (in x- and z-direction) generated higher impact force for the buck model compared to that for the vehicle model. Due to this difference in impact force, pelvis positive deformation (compression) and femur bending moment were both higher for the buck model relative to that for the vehicle model. This can be caused by difference in material property of the grille and hood between the vehicle and buck models.

Phase-IV: Between approximately 42 ms and 55 ms, the magnitude of impact force from the grille was similar between the vehicle and buck models. In this phase, the hood (in x- and z-direction) generated higher impact force for the buck model compared to that for the vehicle model. Due to this difference in impact force, pelvis positive deformation (compression) and femur bending moment were both higher for the buck model relative to that for the vehicle model. This can be attributed to difference in material property of the hood between the vehicle and buck models.

Difference in effect of velocity change As presented in the RESULTS section, a larger difference in pelvis deformation between the vehicle and buck models was seen when impact velocity was changed from 20 km/h to 40 km/h. As for the femur bending moment, the difference between the vehicle and buck models was more evident when impact velocity was changed from 40 km/h to 60 km/h.

Regarding the difference in peak negative pelvis deformation (tension) due to the change in impact velocity from 20 km/h to 40 km/h, peak deformation was reached in Phase-II as described in the previous sub-sub-section. Difference of change in impact force from the bumper face is crucial because 1) this force was predominant compared to the forces from the bumper lower and grille, and 2) the bumper force applied to the knee and distal femur yields tensile force at the hip joint. The ratio of peak impact force from the bumper face between 20 km/h and 40 km/h was 376 % and 256 % for the buck model and vehicle model, respectively. The larger increase in the peak impact force from the bumper face for the buck model can explain the larger increase in negative pelvis deformation (tension). This can be attributed to the difference in rate sensitivity of material property of the bumper face and/or the difference in the effective mass of the deformed portion of the bumper face.

As for the difference in peak positive femur bending moment due to the change in impact velocity from 40 km/h to 60 km/h, peak bending moment was reached in Phase-III as described in the previous sub-sub-section. In this phase, the ratio of peak impact force between 40 km/h and 60 km/h for the hood in x- and z-direction and the grille in x-direction were all larger with the vehicle model than with the buck model. Since this does not explain the difference in the change of peak positive femur bending moment (larger change with the buck model), other factors must be involved. A possible explanation would be the difference in deformed shape of the hood and grille. At 60 km/h, the foam material representing the stiffness characteristics of the hood and grille of the buck model bottomed out, resulting in concentrated impact forces applied to the thigh from the hood leading edge and upper part of the grille. In contrast, the hood and grille of the vehicle model provided much more distributed loads to the thigh. Since a distributed load yields less maximum bending moment relative to a concentrated load, the difference in load distribution level can explain the more significant increase in femur bending moment with the buck model than that with the vehicle model. This can be attributed to the difference in crash stroke of the hood and grille up to bottoming between the vehicle and buck models.

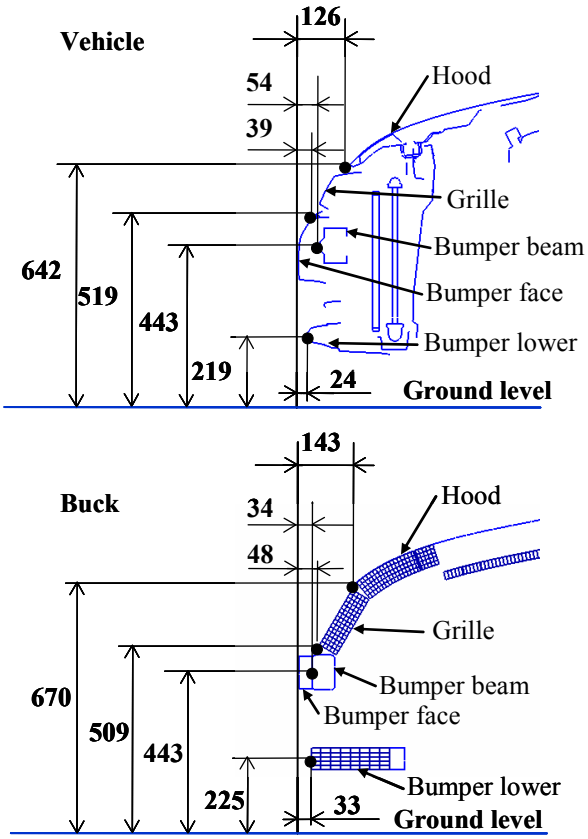

Figure 10. Geometry of vehicle and buck models.

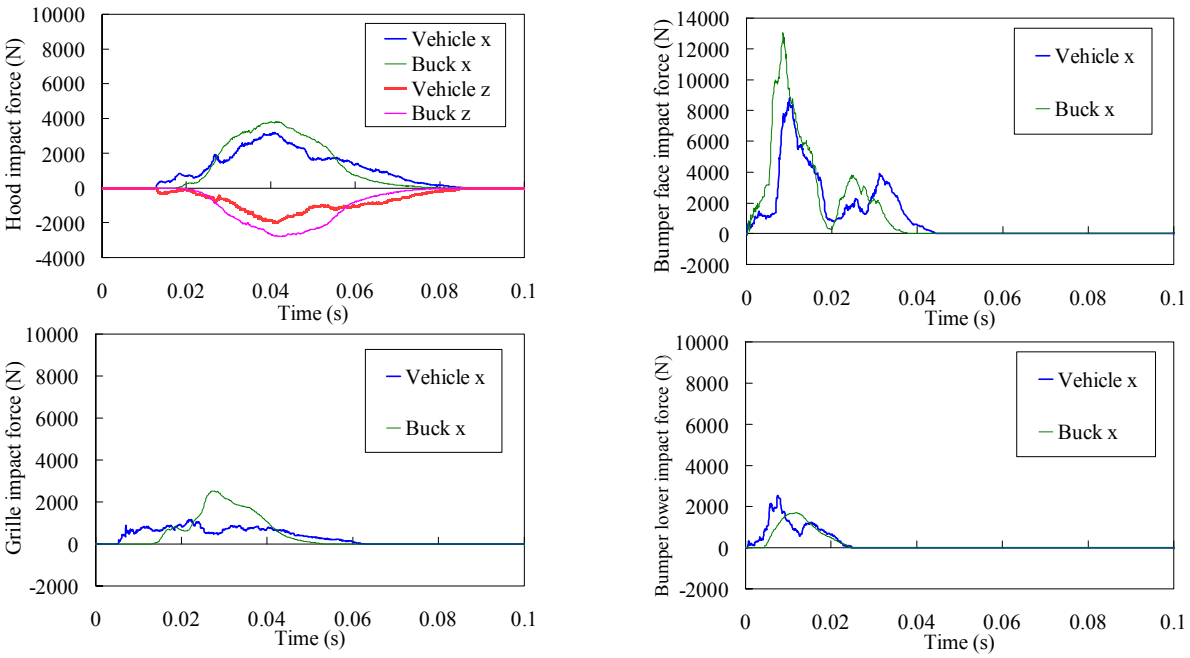

Figure 11. Comparison of impact forces between vehicle and buck models.

Table 2 . Suggested modifications to buck components

Components	Design parameters			Effect on injury parameters
	Geometry	Material	Structure	
Hood		Decreased stiffness		Pelvis positive deformation Femur positive bending moment in phase III and IV
			Increased crash stroke	Femur positive bending moment at velocity change from 40 km/h to 60 km/h
Grille	Front end of grille to be located 9 mm forward			Pelvis deformation from negative to positive Femur bending moment from negative to positive MCL tensile strain in phase II
		Decreased stiffness		Pelvis positive deformation Femur positive bending moment in phase III
			Increased crash stroke	Femur positive bending moment at velocity change from 40 km/h to 60 km/h
Bumper face	Front end of bumper beam to be located 20 mm backward	Decreased stiffness	Decreased stiffness	MCL tensile strain Tibia positive bending moment at phase II
		Less rate-sensitive material	Decreased effective mass	Pelvis negative deformation at velocity change from 20 km/h to 40 km/h
Bumper lower	Front end of bumper lower to be located 9 mm forward			MCL tensile strain at phase I
		Increased stiffness	Increased stiffness	MCL tensile strain at phase II

Suggested modification items for buck components To enhance reproducibility of interaction with a pedestrian relative to the actual vehicle, suggested modifications to the buck components obtained from the analysis described in the previous sub-sub-section are summarized in Table 2. The reasons for the suggestions are also summarized in Table 2 from a viewpoint of difference in responses of injury parameters. Although the results from the impact simulations using the buck model were in general agreement with those from the vehicle model in terms of injury parameters and kinematics, these suggested modifications to the buck model would provide an enhanced representation of pelvis and lower limb injury parameter responses when impacted by an actual vehicle.

FUTURE WORK

In this study, the buck designed to represent a mid-sized sedan was validated. Due to low profile of the front end geometry of the vehicle, all the impact simulations using the vehicle and buck models resulted in only small pelvis deformation. In order to develop a standardized vehicle model for investigating biofidelity of anthropomorphic tools for evaluating pelvis injuries, bucks representing vehicles with higher bonnet leading edge such as SUVs or minivans that would yield larger pelvis deformation need to be developed.

CONCLUSIONS

In this study, a buck model developed in a previous study was validated against a vehicle model represented by the buck by performing impact simulations using a human FE model. Injury parameters on the pelvis and lower limb along with trajectories of each body region were compared between the vehicle and buck models at various impact velocities.

As a result of comparisons of injury parameters and kinematics, it was found that the buck results generally represent injury and kinematic responses of a pedestrian when impacted by the mid-sized sedan. In order to enhance representation of responses of pelvis and lower limb injury measures, it was also found that the following items are suggested to be modified;

1) Geometry of the grille, bumper face and bumper lower
2) Stiffness of the hood, grille, bumper face and bumper lower
3) Rate sensitivity and effective mass of the bumper face
4) Crash stroke of the hood and grille

REFERNCES

[1] International Traffic Safety Data and Analysis Group Data Sets, http //internationaltransportforum.org/irtad/pdf/roaduse.pdf

[2] Y. Mizuno. 2005, "Summary of IHRA Pedestrian Safety WG Activities – Proposed Test Method to Evaluate Pedestrian Protection Afforded by Passenger Cars", *Paper 05-0138, Proceedings of the 19th Conference on the Enhanced Safety Vehicle (ESV)*

[3] Brian J. Eastridge, and Andrew R. Burgess, 1997, "Pedestrian Pelvis Fractures : 5-year Experience of a Major Urban Trauma Center", *The Journal of TRAUMA, Volume 42(4), April 1997, pp. 695-700*

[4] J. G. Snedeker, M. H. Muser and F. H. Walz. 2003, "Assessment of Pelvis and Upper Leg Injury Risk in Car-Pedstrian Collisions: Comparison of Accident Statics, Impactore Tests and a Human Body Finite Element Model", *Stapp Car Crash Journal, Vol 47 (October 2003), pp.437-457*

[5] J. G. Snedeker, F. H. Walts, M. H. Muser and C. Lanz. 2005 "Assessing Femur and Pelvis Injury Risk in Car-Pedestrian Collision: Comparison of Full Body PMTO Impacts, and a Human Body Finte Element Model", *Paper 05-0103, Proceedings of the 19th Conference on the Enhanced Safety Vehicle (ESV)*

[6] Y. Takahashi, S. Suzuki, M. Ikeda and Y. Gunji. 2010, "Investigation on Pedestrian Loading Mechanisms using Finite Element Simulations", *International Research Council on the Biomechanics of Impact (IRCOBI)*

[7] C. Untaroiu, J. Shin, J. Crandall, R. Fredriksson, O. Bostrom, Y. Takahashi, A. Akiyama, M. Okamoto and Y. Kikuchi. 2009, "Development and Validation of Pedestrian Sedan Buck using Finite Element Simulations: Application in Study in the Influence of Vehicle Automatic Breaking on the Kinematics of the Pedestrian Involved in Vehicle Collisions", *Paper 09-0485. Proceedings of the 21th Conference on the Enhanced Safety Vehicle (ESV)*

[8] A. Akiyama, M. Okamoto and N. Rangarajan. 2001, "Development and Application of New Pedestrian Dummy", *Paper 463*, *Proceedings of the 17th Conference on the Enhanced Safety Vehicle (ESV)*

[9] Y. Kikuchi, Y. Takahashi and F. Mori. 2006, "Development of a Finite Element Model for a Pedestrian Pelvis and Lower Limb", *SAE World Congress, paper Number 2006-01-0683*

[10] R. S. Salzar, D. Genovese, C. R. Bass, J. R. Bolton, H. Guillemot, A. M. Damon and J. R. Crandall. 2008, "Load Path Distribution within the Pelvic Structure under Lateral Loading", *International Crashworthiness Conference*

[11] M. Ikeda and Y. Takahashi. 2010, "Investigation on Pelvis Injury Indices Using a Human Finite Element Model", *SAE World Congress, Paper Number 2010-01-1169*

[12] J2868, "Pedestrian Dummy Full Scale Test Results and Resource Materials" *Surface Vehicle Information Report, Society of Automobile Engineers (SAE)*